

Supplementary Material

Results

Subject information

Table S1: Subject information.

ID	Age	Sex	DD (y)	LEDD (mg)	Preoperative UPRDS-III (OFF, ON levodopa; A.U.)	DBS lead model	STN-DBS amplitude (mA)	12MFU UPRDS-III (OFF, ON STN-DBS; A.U.)	ECoG model	ECoG hemi- sphere
EL003	56	F	15	600	31, 18	MT 3389	N/A	N/A	AT TS06R- AP10X- 0W6	L
EL004	45	F	2	1462	n.a.	BS Vercise Cartesia	N/A	N/A	AT TS06R- AP10X- 0W6	L
EL006	57	M	6	1000	31, 11	MT SenSight Short	L: N/A, R: 2.0	57, 24	AT TS06R- AP10X- 0W6	R
EL007	55	M	3	850	36, 9	MT SenSight Short	L: 2.0, R: 1.5	48, 35	AT DS12A- SP10X- 000	R
EL008	66	M	8	858	59, 28	BS Vercise Cartesia X	N/A	N/A	AT TS06R- AP10X- 0W6	L
EL009	59	M	7	1600	24, 8	MT SenSight Short	L: 2.0, R: 2.0	35, 11	AT TS06R- AP10X- 0W6	L
EL010	66	F	12	900	27, 11	MT SenSight Short	N/A	N/A	AT TS06R- AP10X- 0W6	R
EL011	67	M	7	949	30, 9	MT	N/A	N/A	AT	R

						SenSight Short			TS06R- AP10X- OW6	
EL012	54	M	12	866	39, 14	MT SenSight Short	L: 1.5, R: 1.5	43, 18	AT TS06R- AP10X- OW6	R
EL013	64	M	9	800	31, 12	MT SenSight Short	N/A	N/A	AT DS12A- SP10X- 000	R
EL014	52	M	14	1750	35, 8	MT SenSight Short	L: 2.0, R: 2.5	52, 32	AT TS06R- AP10X- OW6	R
EL016	73	M	20	1630	47, 19	MT SenSight Short	N/A	N/A	AT TS06R- AP10X- OW6	R
EL017	65	F	8	1150	41, 14	MT SenSight Short	L: 3.0, R: 2.0	n.a.	AT TS06R- AP10X- OW6	R
EL019	58	M	10	1215	39, 18	MT SenSight Short	L: N/A, R: 2.5	n.a.	AT TS06R- AP10X- OW6	R
EL020	51	M	7	880	32, 24	MT SenSight Short	N/A	N/A	AT TS06R- AP10X- OW6	R
EL021	43	M	10	1000	42, 23	MT SenSight Short	N/A	N/A	AT TS06R- AP10X- OW6	R
EL022	70	M	7	1073	41, 23	MT SenSight Short	L: 3.0, R: 3.0	n.a.	AT TS06R- AP10X- OW6	R
EL023	67	M	8	1700	44, 20	MT SenSight Short	L: 2.5, R: 2.5	n.a.	AT TS06R- AP10X-	R

Abbreviations: AT – Ad-Tech; BS – Boston Scientific; DBS – deep brain stimulation; DD – disease duration; ECoG – electrocorticography; F – female; L – left; LEDD – levodopa-equivalent daily dose; M – male; MT – Medtronic; N/A – not applicable; n.a. – not available; R – right; STN - subthalamic nucleus; UPDRS - Universal Parkinson's Disease Rating Scale; 12MFU – 12-month follow up post-implantation. Note that preoperative UPDRS-III scores were unavailable for subject EL004. Note that 12MFU UPDRS-III scores were unavailable for subjects EL017, EL019, EL022, and EL023.

Spatial maps of local power

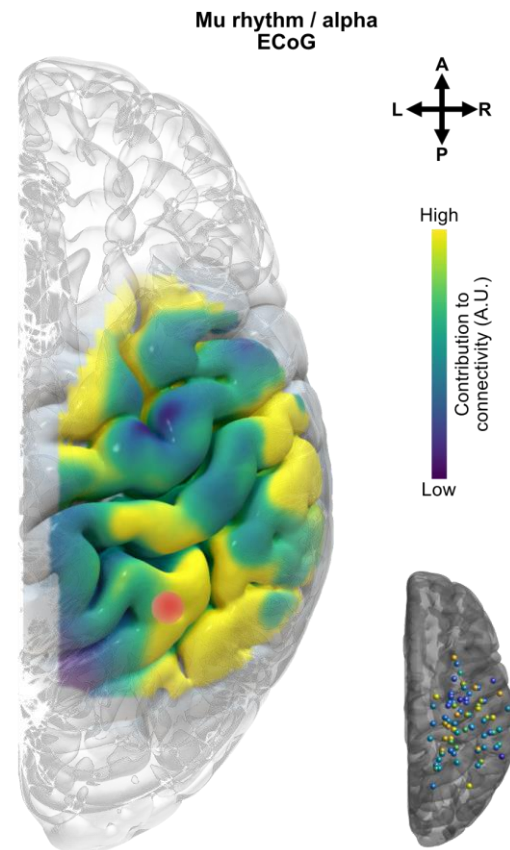


Figure S1: Spatial maps of local power. Localisation of the strongest power component extracted with spatio-spectral decomposition for cortical mu rhythm/alpha, averaged over OFF therapy and ON levodopa. Localisations are shown for individual electrodes and interpolated to surfaces. Red dot shows point of strongest source. Abbreviations: A – anterior; ECoG – electrocorticography; L – left; P – posterior; R – right.

Directed sensory cortex – STN communication

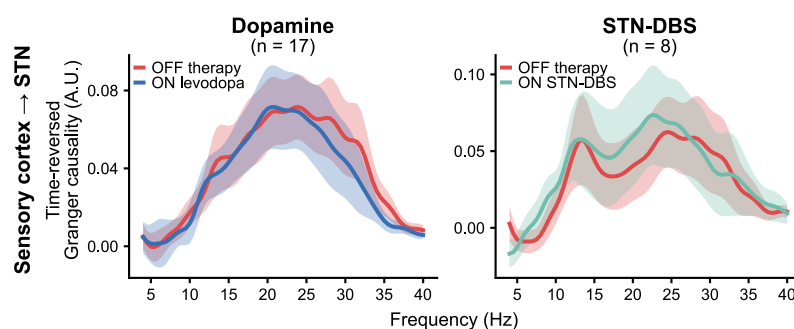


Figure S2: Sensory cortex – STN directed communication. Granger causality shows sensory cortex drives communication with STN across medication and stimulation states. Shaded coloured areas show standard error of the mean. Abbreviations: DBS – deep brain stimulation; STN – subthalamic nucleus.

Directionality of cortico-subthalamic communication OFF therapy vs. ON STN-DBS

Time-reversed Granger causality (TRGC) revealed the driving force of communication from motor cortex to STN was reduced in the high beta band with STN-DBS (Figure 3C; Figure S3G). Given that TRGC is based on net Granger scores, this reduction with stimulation can reflect: 1) reduced information flow from cortex to STN; 2) increased information flow from STN to cortex; or 3) a combination of 1 and 2. To assess which scenario is responsible for the observed change, we can examine the various Granger scores used to compute TRGC. Following the notation of Winkler et al.¹: X is defined to be the motor cortex seeds, and Y the STN targets; $F_{X \rightarrow Y}$ and $F_{Y \rightarrow X}$ are the Granger scores from seeds to targets and targets to seeds, respectively; $F_{X \rightarrow Y}^{\text{net}}$ is the difference of Granger scores (i.e. $F_{X \rightarrow Y} - F_{Y \rightarrow X}$); \sim represents time-reversal of signals; and finally, $\tilde{D}_{X \rightarrow Y}^{\text{net}}$ is TRGC (i.e. $F_{X \rightarrow Y}^{\text{net}} - \tilde{F}_{\tilde{X} \rightarrow \tilde{Y}}^{\text{net}}$).

First, $F_{X \rightarrow Y}$ reveals high beta information flow from cortex to STN to be reduced with stimulation (scenario 1; Figure S3A), and strongly resembles the final TRGC scores (Figure S3G). Second, $F_{Y \rightarrow X}$ shows increased information flow from STN to cortex with stimulation from 30 Hz (scenario 2; Figure S3B). Together, these findings would suggest that the change in cortical driving force with stimulation reflects both reduced information flow from cortex and increased information flow from STN (scenario 3). However, the increased information flow from STN to cortex with stimulation from 30 Hz is also present in the time-reversed signals, as $\tilde{F}_{\tilde{Y} \rightarrow \tilde{X}}$ shows (Figure S3E). Given that the purpose of time-reversal is to capture weak data asymmetries – properties of the data which do not reflect causal interactions between signals² – we attribute the increased information flow from STN to cortex with stimulation from 30 Hz as ‘noise’, potentially a residual stimulation artefact given that it continues to ramp towards the stimulation frequency (130 Hz). In contrast, $\tilde{F}_{\tilde{X} \rightarrow \tilde{Y}}$ shows a lack of difference in the high beta band between stimulation conditions (Figure S3D), indicating that the reduced information flow from cortex to STN with stimulation is not the result of weak data asymmetries. Altogether, we attribute the reduced cortical high beta driving force observed in the final TRGC scores to a reduction of information flow from cortex to STN (scenario 1), and not an increase of information flow from STN to cortex.

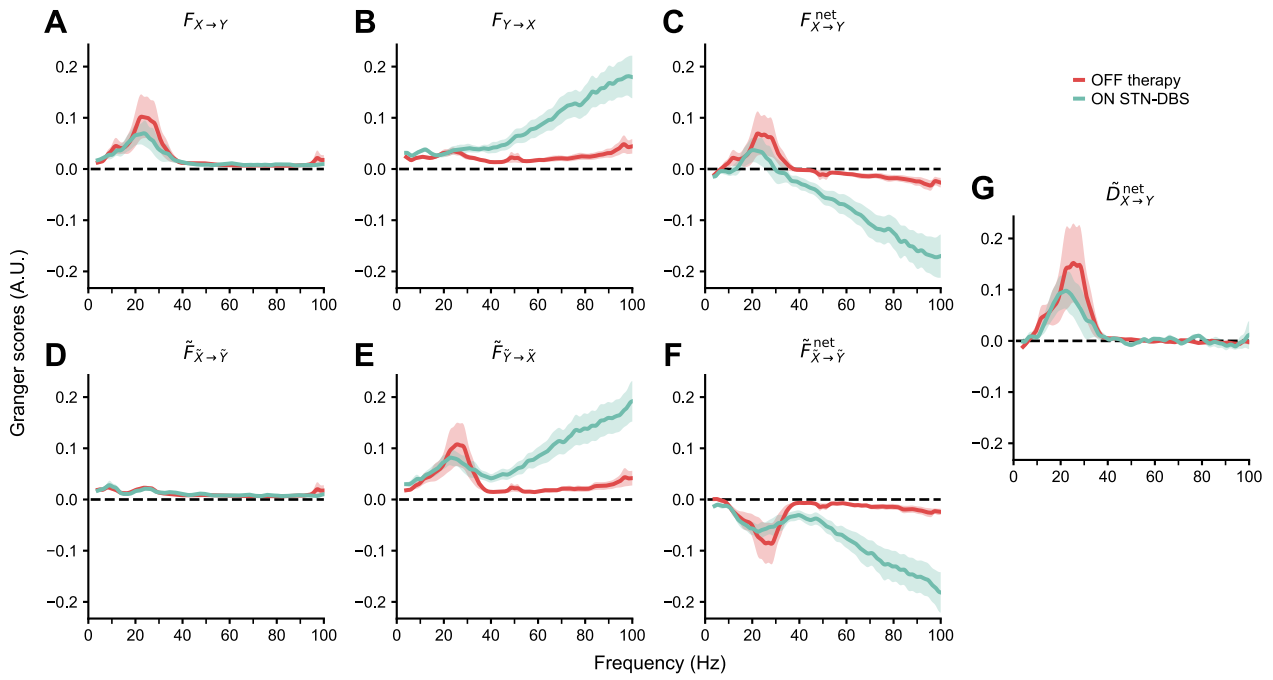


Figure S3: Directionality of cortico-subthalamic connectivity. We define X to be motor cortex ECoG signals, and Y to be STN-LFP signals. (A) Granger scores from motor cortex to STN. (B) Granger scores from STN to motor cortex. (C) Net Granger scores from motor cortex to STN. (D) Granger scores of time-reversed signals from motor cortex to STN. (E) Granger scores of time-reversed signals from STN to motor cortex. (F) Net Granger scores of time-reversed signals from motor cortex to STN. (G) Time-reversed Granger causality from motor cortex to STN. Shaded coloured areas show standard error of the mean.

Spatial maps of cortico-subthalamic coupling

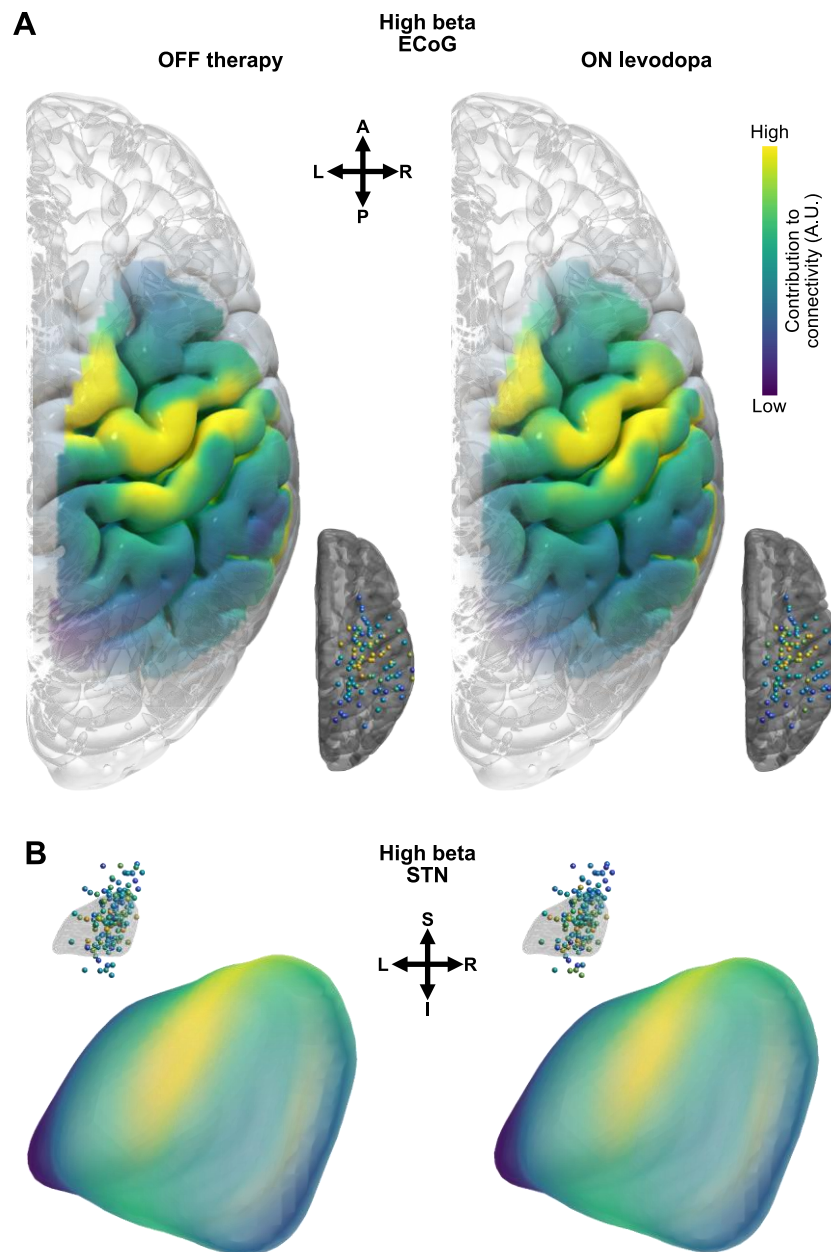


Figure S4: Spatial maps of cortico-subthalamic coupling. Spatial contribution maps from the maximised imaginary coherency analysis reveals (A) motor cortex and (B) dorsolateral STN as the strongest contributors to high beta connectivity OFF therapy and ON levodopa. Localisations are shown for individual electrodes and interpolated to surfaces. Abbreviations: A – anterior; ECoG – electrocorticography; I – inferior; L – left; P – posterior; R – right; S – superior; STN – subthalamic nucleus.

References

1. Winkler, I., Panknin, D., Bartz, D., Müller, K.-R., and Haufe, S. (2016). Validity of time reversal for testing Granger causality. *IEEE Trans. Signal Process.* 64, 2746–2760.
2. Haufe, S., Nikulin, V.V., and Nolte, G. (2012). Alleviating the influence of weak data asymmetries on granger-causal analyses. In *Latent Variable Analysis and Signal Separation: 10th International Conference, LVA/ICA 2012, Tel Aviv, Israel, March 12-15, 2012. Proceedings 10* (Springer), pp. 25–33.